Bend monitoring and refractive index sensing using flat fibre and multicore Bragg gratings

OPEN ACCESS
IOP Publishing
Measurement Science and Technology
Meas. Sci. Technol. **31** (2020) 085203 (6pp)
https://doi.org/10.1088/1361-6501/ab8710

Bend monitoring and refractive index sensing using flat fibre and multicore Bragg gratings

Christopher Holmes[1], Sumiaty Ambran[2], Peter A Cooper[1], Andrew S Webb[1], James C Gates[1], Corin B E Gawith[1], Jayanta K Sahu[1] and Peter G R Smith[1]

[1] Optoelectronics Research Centre, University of Southampton, Southampton SO17 1BJ, United Kingdom
[2] Malaysia–Japan International Institute of Technology, Universiti Teknologi Malaysia, Kuala Lumpur, Malaysia

E-mail: christopher.holmes@soton.ac.uk

Received 28 January 2020, revised 1 April 2020
Accepted for publication 6 April 2020
Published 25 May 2020

Abstract

A planarized optical fibre designed for two-dimensional bend monitoring and external refractive index sensing is presented. The approach uses two single-mode waveguides each containing a set of spectrally multiplexed Bragg gratings. To achieve sensitivity to bending and external refractive index, the cladding material of the fibre is partially removed through physical machining. This acts to offset the neutral axis, increasing bend sensitivity, and exposes the evanescent field of the guided mode, permitting external refractive index monitoring. Through collective monitoring of the Bragg grating array, real time, multiparameter sensing is attainable, allowing new capability for intelligent monitoring.

Keywords: optical fibre, Bragg gratings, multicore fibre, planar optics, bend sensing

(Some figures may appear in colour only in the online journal)

1. Introduction

Intelligent monitoring of engineered structures and materials is enabled by increasing both the number of sensor elements and the capability of the sensor technology [1]. Optical fibre sensors have specific advantages when applied to intelligent monitoring as they have: immunity to electromagnetic interference; are lightweight; have a small cross-sectional footprint; broad spectral bandwidth; remote and secure connectivity and use materials that are typically chemically inert and non-conductive. Multiparameter optical fibre sensors are an enabler for intelligent monitoring, as they provide an increased sensor capability. They have been the subject of considerable research in recent years [2] as they can additionally improve the accuracy and precision of multi-variant system measurements. For example, through simultaneous temperature monitoring, refractive index sensing can be thermally compensated improving accuracy and precision. Previous work on multiparameter optical fibre bend monitoring has included multicore fibre [3, 4] and regular fibre adhered to larger cantilevered structures. In both instances the neutral axis is offset from a waveguide core to make it optically responsive to bending. Multiparameter bend monitoring has also been demonstrated in flexible planar optical platforms, notably silica [5, 6], polymer [7], chalcogenide [8–10] and silicon [11]. In these configurations strain is mapped for a two-dimensional plane.

The work reported here uniquely considers a flexible planar optical fibre platform, termed flat fibre [12], illustrated in figure 1. Flat fibre provides both long flexible lengths associated with optical fibre and the functionality of planar optics. Recent applications for flat fibre have included refractometry and dosimetry. Refractometry has included guided mode [13], leaky mode [14] and plasmon coupling [15, 16] techniques. Dosimetry has included *in-vivo* applications, through use of

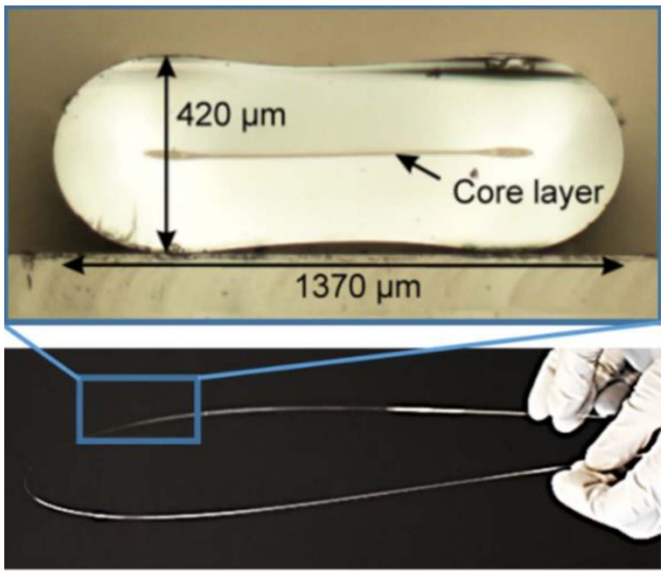

Figure 1. Flexible flat optical fibre, illustrating the planar cross-section (top) and inherent flexibility (bottom).

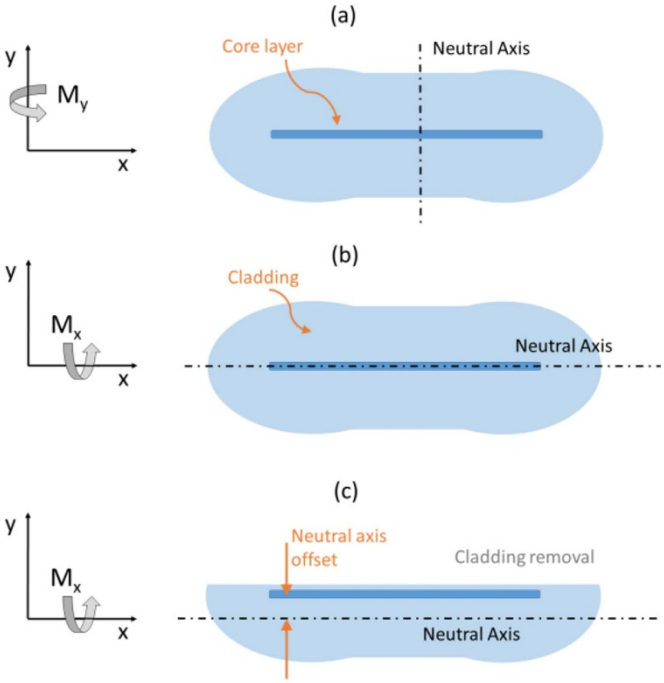

Figure 2. Neutral axis locations in flat fibre (cross section) for (a) bending moments about the *y*-axis, (b) bending moments about the *x*-axis, (c) bending moments about the *x*-axis, with partial removal of clad material removed.

thermoluminescence [17, 18]. None of this work has yet considered bend monitoring or utilisation of multiparameter sensing.

Flat fibre is an inherent slab waveguide, laterally multimode and vertically single mode [12]. Through use of physical micromachining [19], Direct UV writing (DUW) [13] or femtosecond laser writing [20, 21] these multimode characteristics can be manipulated. Through direct laser writing (either DUW or femtosecond writing) multiple single-mode waveguides can be arbitrarily positioned into the core layer of flat fibre. In this instance flat fibre shares similarity to solid multicore fibre [22], with the distinguishing advantage of integrated circuitry [23].

This report describes the design, fabrication and response of a flat fibre capable of multiparameter sensing, namely monitoring two-dimensional bending, external refractive index and temperature. Bend sensitivity of flat fibre is directly compared to multicore cylindrical fibre through replicating dual-axis bending described by Flockhart *et al* [24].

2. Design concept and fabrication

Flat fiber is fabricated using modified chemical vapour deposition (MCVD) and fiber drawing. The process differs from standard optical fibre fabrication only at the drawing stage, where a vacuum is applied to the preform in order to preferentially collapse it into a planar geometry. A cross-section of the resulting fibre is shown in figure 1.

The strain observed in the core layer of flat fibre is dependent upon the bending moments applied and relative position from the neutral axis. For bending moments about the *y*-axis, M_y, the neutral axis is located upon the plane of symmetry, as shown in figure 2(a). For bending moments about the *x*-axis, M_x, the neutral axis overlaps with the core layer, illustrated in figure 2(b). This means that for bending in the *x*-axis there is minimal strain observed in the core. The partial removal of cladding material on one side of the flat fibre acts to offset the neutral axis, as shown in figure 2(c), meaning strain-induced bending for the M_x can be observed. Further to this, complete removal of clad material will permit evanescent field exposure of the guided modes, which can be leveraged to probe external refractive index.

To offset the neutral axis cladding material was removed through physical machining, achieved through post process lapping and polishing (using a Logitech LP50). The physical machining process allowed a small wedge angle of 0.27° between the top and bottom of the fibre, shown in figure 3(a). This meant that the overclad thickness varied from 105 µm at the thickest end to complete removal of the core layer at the opposite end. It also meant that part of the flat fibre was evanescently exposed to its external environment.

To allow fibre bending, refractive index and temperature measurements, two waveguides containing an array of spectrally multiplexed Bragg gratings were defined, as outlined in figure 3(b). The waveguides and Bragg gratings were written into the photosensitive germanium-doped core layer of the flat fibre, through use of small spot direct UV writing [25]. Here, a 244 nm frequency doubled argon-ion laser is used to increase the local refractive index in the core layer. A 6 µm spot consisting of two coherent beams focused and overlapping are translated through the fibre. The dual beams create an inherent interference pattern, which was amplitude modulated during translation in order to define the outlined array of multiplexed Bragg gratings and waveguides. Through use of a commercial optical backscatter reflectometer (Luna, OBR

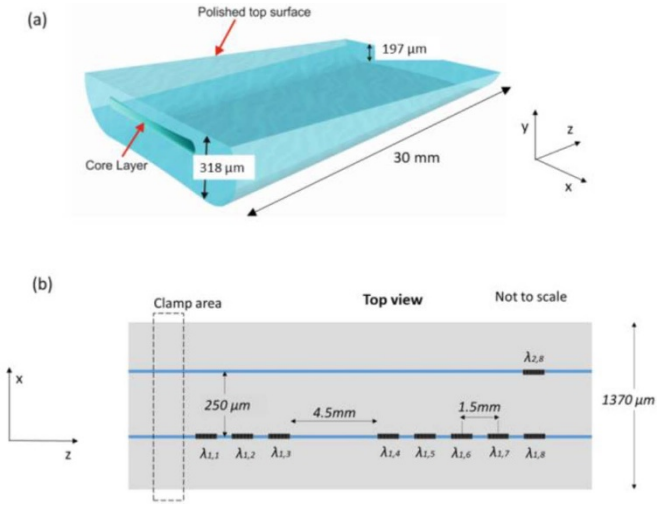

Figure 3. Configuration of physically machined flat fibre showing (a) the location of direct UV written waveguides and Bragg gratings and (b) the machined wedge used to shift the neutral axis.

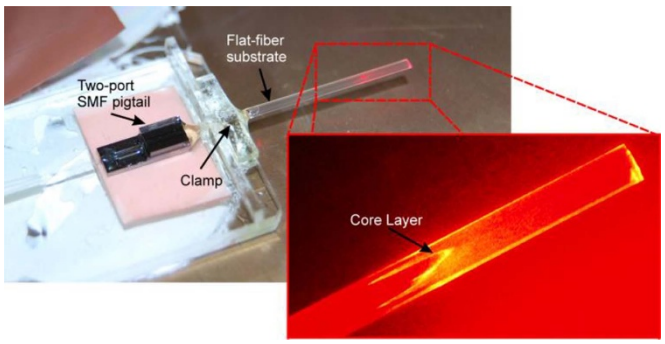

Figure 4. Flat fibre cantilevered section, showing optical coupling of 633 nm laser light.

4400 series) waveguide propagation loss was measured to be 0.09 ± 0.01 dB cm^{-1}.

Direct UV writing of the waveguides and gratings were made prior to the physical machining of the fibre. The two straight waveguides defined were offset by 125 µm and centred about the vertical neutral axis (i.e. 250 µm from each other), shown in figure 3(b).

3. Bend sensitivity of flat fibre

Bending of the flat fibre was induced through leveraging it as a cantilever. The arrangement clamped the thickest end of fibre, with packed borosilicate slides and epoxy, as illustrated in figure 4. Light was coupled into the two flat fibre waveguides using two single-mode fibres (SMFs). The arrangement used a two-port SMF pigtail, consisting of two silicon v-grooves of pitch 250 µm (OzOptics).

The cantilevered arrangement was clamped down and deflected at the end about *y*-axis and *x*-axis respectively. This was achieved using a lever and multi-axis micrometre translation stages, as illustrated in figure 5(a). The Bragg gratings in each waveguide were simultaneously addressed using two

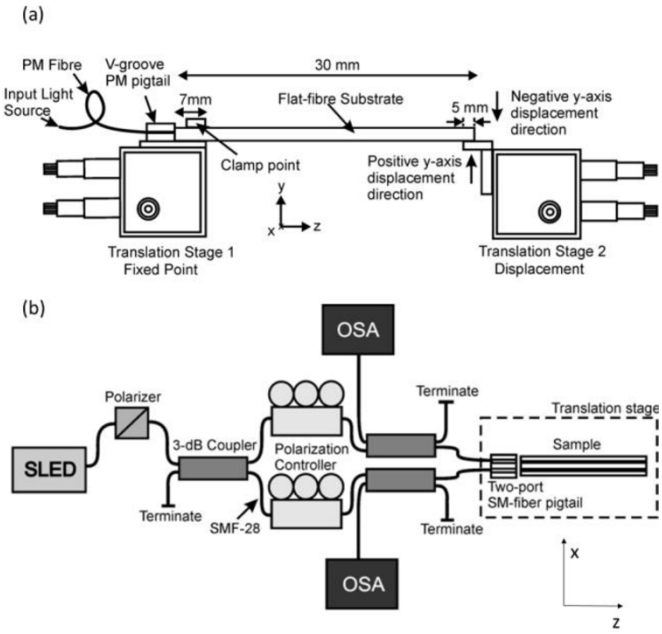

Figure 5. Bend test set-up, showing (a) translation stage arrangement and (b) optical characterisation set-up.

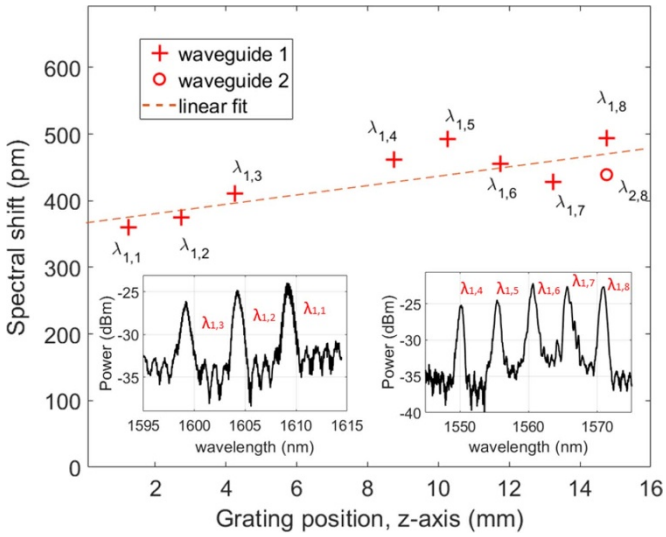

Figure 6. Spectral response for Bragg gratings along the length of flat optical fibre, upon a distal end deflection of 1 mm in the *y*-axis, (inserts) corresponding reflection spectra from gratings.

Optical Spectrum Analysers, OSAs (ANDO AQ6317B) and a 5-element superluminescent LED broadband source (Amonics ASLD-CWDM-5-B-FA), using the configuration shown in figure 5(b). Back reflected spectral signatures are presented in figure 6.

To theoretically corroborate the optical response, the strain induced in flat fibre was modelled through finite element analysis (FEA) (Comsol Multiphysics, Solid Mechanics). This considered all three orthogonal linear strain components [5].

Figure 6 depicts the measured spectral response for the Bragg grating array, subjected to a -1 mm *y*-axis deflection.

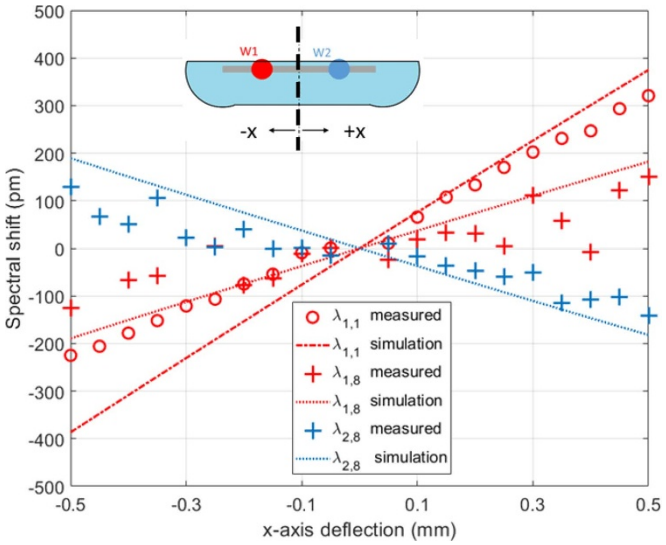

Figure 7. Spectral response of Bragg gratings at the root and distal end of flat fibre subjected to calibrated deflections in the *x*-axis.

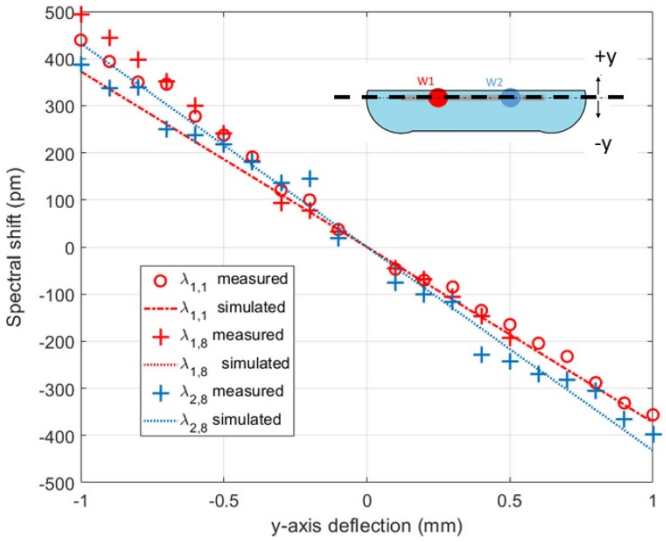

Figure 8. Spectral response of Bragg gratings at the root and distal end of flat fibre subjected to calibrated deflections in the *y*-axis.

Table 1. Summarised bend sensitivity.

Bragg grating	*x*-axis deflection (pm mm^{-1})	*y*-axis deflection (pm mm^{-1})
$\lambda_{1,1}$	280 ± 50	-400 ± 40
$\lambda_{1,8}$	641 ± 5	-490 ± 50
$\lambda_{2,8}$	-240 ± 10	-387 ± 3

Here, grating position is referenced with respect to the cantilever's root. Unlike a cantilever of uniform cross section where maximum strain would occur at the root, this cantilever has variable cross-section thus a varying neutral axis and stiffness along the length. This means that the maximum spectral shift occurs at the distal end of the cantilever, observed both experimentally and with FEA simulations.

Figures 7 and 8 show the Bragg responses for gratings at the distal end and root of the cantilever, subjected to *x*-axis and *y*-axis displacements. Experimental observations are in good agreement with theoretical simulation. However, response asymmetries about zero-deflection exist. This is believed to result from a small variation of thickness along the *x*-axis. It should be noted that this would be most notable for *x*-axis deflection due to a neutral axis offset, as indeed observed. Bend sensitivity for the Bragg gratings are summarised in table 1. A maximum of 641 ± 5 pm mm^{-1} occurs for positive deflections about the *x*-axis, inferred from 10 data points. This is approximately an order of magnitude larger in spectral shift when compared to similar work on multicore optical fibre [24]. It is noted that the neutral axis offset is approximately 6 times larger in this work and therefore a larger spectral response is indeed expected.

The thermo-optic response for the Bragg gratings was calibrated from 22 °C to 58 °C, using a hotplate (Fisher Scientific, Isotemp) and K-type thermocouple. Thermal sensitivity was measured to be 8.5 ± 0.6 pm K^{-1} for the evanescent exposed ($\lambda_{2,8}$) Bragg grating, and 11.6 ± 0.7 pm K^{-1} for the none exposed gratings. It is noted that upon the calibration of thermal and bending response of three gratings, temperature can be practically deduced through use of linear simultaneous equations.

4. Refractive index sensitivity of flat fibre

One of the Bragg gratings in the array, $\lambda_{2,8}$, was evanescently exposed and responded to changes in external refractive index. It is noted that due to the secondary wedge along the *x*-axis only this grating displayed such sensitivity. To calibrate the response, the fibre was tested with calibrated refractive index oils (Cargille Series AAA and Series AA). Figure 9 shows the spectral sensitivity of this grating to the fluids.

The Bragg wavelength changes are larger for external refractive indices approaching that of the core layer, a trend understood from solutions to Helmholtz equations [26]. The maximum sensitivity to external refractive index is 20 nm riu^{-1}. It is further observed that in the presence of an external refractive index fluid there is negligible influence on the bend sensitivity, as seen in figure 9 insert. This shows a unique capability of flat fibre to simultaneously monitor strain and external refractive index, distinguishable through differential spectral measurements.

5. Discussion

This work is the first demonstration of combined bend and external refractive index monitoring using flat fibre. The solution reported uses physical machining in the form of lapping and polishing to both shift the neutral axis and gain partial evanescent field exposure. It is noted that other techniques including laser ablation, wet etching, dry etching, ultrasonic milling either post or prior to fibre drawing could also be used to achieve a similar geometric configuration. These would

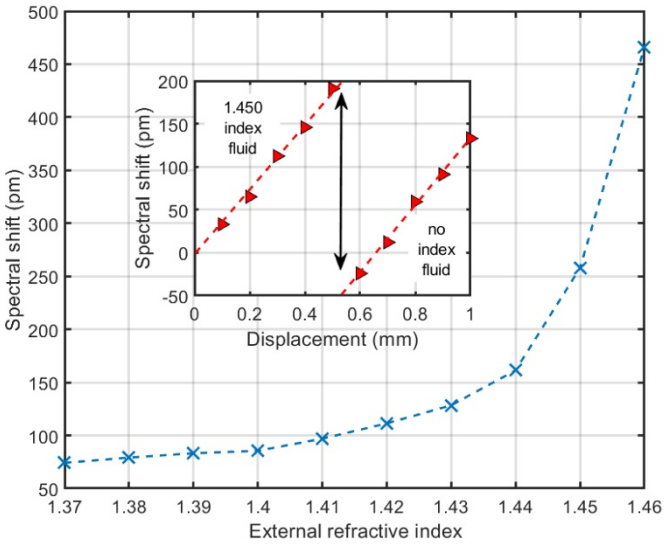

Figure 9. Response of an evanescent field exposed flat optical fibre Bragg grating to Cargille refractive index fluids that are calibrated at 633 nm (insert) vertical bending response of the grating with and without index oil.

be a direction for further development and may offer greater scalability.

Monitoring external refractive index in addition to strain components would provide a unique capability for intelligent monitoring. For example, it could be practically used for monitoring degradation of epoxy resin [27, 28] such as that found within advanced composites (e.g. carbon fibre reinforced polymer). This capability could be set alongside traditional Bragg grating strain monitoring capability achieved through embedding optical flat fibre. Applications could also include physical and refractive index monitoring of fluids, which could be used to infer directional fluid flow (through cantilever deflection) and density (through external refractive index).

Flat fibre has an asymmetric stiffness inherent to its geometry. This limits complex three-dimensional shape sensing, as demonstrated in multicore optical fibre [3, 29]. However, the platform could be embedded within advanced composites or upon a planar surface. Investigation into long-term performance and durability under suitable strain transfer [30] would be required and the subject of future investigation.

6. Conclusion

This is the first report of multi-parameter sensing within flat fibre. The platform demonstrates two-dimensional bend sensitivity and combined external refractive index monitoring and temperature sensing.

The measured bend sensitivity concurs with theoretical models and is enabled through physical machining of the fibre. A maximum bend sensitivity of 641 $\pm$ 5 pm mm^{-1} was measured and external refractive index sensitivity of 20 nm riu^{-1}.

Flat fibre enables multiparameter sensing capability, through which data-rich information can be generated with potential application for future intelligent monitoring applications.

Acknowledgments

Engineering and Physical Sciences Research Council (EPSRC) (EP/M013294/1, EP/M024539/1).

ORCID iDs

Christopher Holmes https://orcid.org/0000-0001-9021-3760
Sumiaty Ambran https://orcid.org/0000-0002-8851-1977
James C Gates https://orcid.org/0000-0001-8671-5987
Corin B E Gawith https://orcid.org/0000-0002-3502-3558
Peter G R Smith https://orcid.org/0000-0003-0319-718X

References

[1] McEvoy M A and Correll N 2015 Materials that couple sensing, actuation, computation, and communication *Science* **347** 1328–37
[2] Pevec S and Donlagić D 2019 Multiparameter fiber-optic sensors: a review *Opt. Eng.* **58** 1
[3] Moore J P and Rogge M D 2012 Shape sensing using multi-core fiber optic cable and parametric curve solutions *Opt. Express* **20** 2967
[4] Cranch G A, Flockhart G M H, MacPherson W N, Barton J S and Kirkendall C K 2006 Ultra-high-sensitivity two-dimensional bend sensor *Electron. Lett.* **42** 9
[5] Holmes C, Carpenter L G, Rogers H L, Gates J C and Smith P G R 2011 Quantifying the optical sensitivity of planar Bragg gratings in glass micro-cantilevers to physical deflection *J. Micromech. Microeng.* **21** 035014
[6] Holmes C, Carpenter L G, Gates J C and Smith P G R 2012 Miniaturization of Bragg-multiplexed membrane transducers *J. Micromech. Microeng.* **22** 025017
[7] Missinne J *et al* 2018 Bragg-grating-based photonic strain and temperature sensor foils realized using imprinting and operating at very near infrared wavelengths *Sensors* **18** 1–14
[8] Hu J, Li L, Lin H, Zhang P, Zhou W and Ma Z 2013 Flexible integrated photonics: where materials, mechanics and optics meet [Invited] *Opt. Mater. Express* **3** 1313
[9] Li L *et al* 2018 Monolithically integrated stretchable photonics *Light Sci. Appl.* **7** 17138
[10] Li L *et al* 2017 A new twist on glass: a brittle material enabling flexible integrated photonics *Int. J. Appl. Glass Sci.* **8** 61–68
[11] Fan L, Varghese L T, Xuan Y, Wang J, Niu B and Qi M 2012 Direct fabrication of silicon photonic devices on a flexible platform and its application for strain sensing *Opt. Express* **20** 20564
[12] Dambul K D *et al* 2019 Fabrication and characterization of Ge-doped flat fibres *J. Mod. Opt.* **66** 1219–25
[13] Rafiq F *et al* 2012 Direct UV written optical waveguides in flexible glass flat fiber chips *IEEE J. Sel. Top. Quantum Electron.* **18** 1534–9
[14] Yong P S, Chai T D, Meng S Y, Shien Y K, Mahdiraji G A and Adikan F R M 2016 Numerical investigation of single-mode operation flat fiber and dispersion *Proc. Eng.* **140** 95–98
[15] De M and Singh V K 2020 Analysis of a highly sensitive flat fiber plasmonic refractive index sensor *Appl. Opt.* **59** 380
[16] Rifat A A, Mahdiraji G A, Sua Y M, Ahmed R, Shee Y G and Adikan F R M 2016 Highly sensitive multi-core flat fiber

surface plasmon resonance refractive index sensor *Opt. Express* **24** 2485
[17] Lam S E, Bradley D A, Mahmud R, Pawanchek M, Abdul Rashid H A and Mohd Noor N 2019 Dosimetric characteristics of fabricated Ge-doped silica optical fibre for small-field dosimetry *Results Phys.* **12** 816–26
[18] Ghomeishi M, Mahdiraji G A, Adikan F R M, Ung N M and Bradley D A 2015 Sensitive fibre-based thermoluminescence detectors for high resolution *in-vivo* dosimetry *Sci. Rep.* **5** 1–10
[19] Ambran S *et al* 2012 Fabrication of a multimode interference device in a low-loss flat-fiber platform using physical micromachining technique *J. Light. Technol.* **30** 2870–5
[20] Kalli K *et al* 2015 Flat fibre and femtosecond laser technology as a novel photonic integration platform for optofluidic based biosensing devices and lab-on-chip applications: current results and future perspectives *Sens. Actuators* B **209** 1030–40
[21] Beecher S J, Thomson R R, Brown G, Webb A S, Sahu J K and Kar A K 2013 Bragg grating waveguide array ultrafast laser inscribed into the cladding of a flat fiber *MATEC Web Conf.* **8** 06001
[22] Richardson D J, Fini J M and Nelson L E 2013 Space-division multiplexing in optical fibres *Nat. Photon.* **7** 354–62
[23] Webb A S *et al* 2007 MCVD planar substrates for UV-written waveguide devices *Electron. Lett.* **43** 1–2
[24] Flockhart G M H, MacPherson W N, Barton J S, Zhang L, Bennion I and Jones J D C 2007 Two-axis bend measurement with Bragg gratings in multicore optical fiber *Opt. Lett.* **28** 387
[25] Holmes C *et al* 2015 Direct UV-written planar Bragg grating sensors *Meas. Sci. Technol.* **26** 112001
[26] Chryssis A N, Lee S M, Lee S B, Saini S S and Dagenais M 2005 High sensitivity evanescent field fiber Bragg grating sensor *IEEE Photonics Technol. Lett.* **17** 1253–5
[27] Marro Bellot C, Olivero M, Sangermano M and Salvo M 2018 Towards self-diagnosis composites: detection of moisture diffusion through epoxy by embedded evanescent wave optical fibre sensors *Polym. Test* **71** 248–54
[28] Kumar T, Singh B G and Nakamura R P 2002 Degradation of carbon fiber-reinforced *J. Compos. Mater.* **36** 2713–33
[29] Mandal K K *et al* 2017 Enhancement of accuracy in shape sensing of surgical needles using optical frequency domain reflectometry in optical fibers *Biomed. Opt. Express* **8** 2210
[30] Wang H, Xiang P and Jiang L 2019 Strain transfer theory of industrialized optical fiber-based sensors in civil engineering: a review on measurement accuracy, design and calibration *Sens. Actuators* A **285** 414–26